A Channel Model for Three-node Two-way Relay-aided PLC Systems

Angie A. G. Liong *, Lenin Gopal *, Filbert H. Juwono *, Choo W. R. Chiong *, and Yue Rong †
* Department of Electrical and Computer Engineering, Curtin University Malaysia, 98009 Miri, Sarawak, Malaysia
†Department of Electrical and Computer Engineering, Curtin University, Perth WA 6845, Australia
Email: angie.liong@postgrad.curtin.edu.my, {lenin, filbert.hilman, raymond.ccw}@curtin.edu.my, y.rong@curtin.edu.au

***Abstract*—A point-to-point (P2P) indoor power line communications (PLC) channel has similar broadcasting nature as the wireless propagation channel because of its tree-like topology. However, once a relay node is introduced into the PLC system, it shows some notable differences between the relay-aided (RA) PLC channels and the wireless channels. In the literature, a channel model for three-node one-way RA PLC system has been discussed. However, three-node two-way PLC system is needed in several applications such as smart grids. Therefore, in this paper, we aim to model the RA PLC system with forward and reverse channels. We use the ABCD method to derive the channel transfer function (CTF) expressions. The CTFs of an RA PLC channel cannot be simply stimulated by cascading two independent P2P channels which can be proved by the simulation results.**

***Index Terms*—Channel transfer function (CTF), power line communications (PLC), relay-aided system**

I. Introduction

A smart grid system is characterized by two-way electricity power and information flows [1]–[3]. With the help of two-way communication links, a smart grid system enables the power control which maximizes the efficiency of electricity generation, transmission and distribution [4]–[6]. Power line communications (PLC) is one of the preferred technology for smart grid communication because power line infrastructure has been available widely so no additional cost is required [7]–[9].

Through the understanding of the PLC channel characteristics, PLC systems can be designed to be more reliable. In the literature, PLC channel models can be grouped into bottom-up and top-down models. In general, bottom-up models are more suitable to use as they use the network information to create a strong connection with the physical topology [10]. Bottom-up channel models utilize the transmission line (TL) theory to obtain the channel transfer function (CTF) using the network structure, cable parameters and appliance impedances [11]. However, the existing PLC channel models are still based on point-to-point (P2P) links.

P2P PLC systems may have some limitations due to the harsh nature of power line channels. Therefore, cooperative communication scheme using relays can be used to improve the system performance. In a broadcast-and-multiaccess (BMA) three-node relay system which consists of one source node, one relay, and one destination, the signal is broadcasted by the source node to the other two nodes in the first phase transmission. In the second phase, the source node continues to broadcast while the relay node forwards its received signal to the destination node. Note that the relay node uses the time-division duplexing (TDD) mode in this scheme [12].

The existing P2P PLC channel models cannot be directly applied to the relay-aided (RA) PLC. It is because the paths are highly correlated due to the use of the same power cables. In the literature, [13] discussed channel modelling of an RA PLC with focus on the general three-node one-way PLC system. However, as previously mentioned, smart grid applications need two-way communication links. To the best of our knowledge, three-node two-way RA PLC channel model has not been discussed in the existing research works. Therefore, in this paper, we aim to model the three-node two-way RA PLC channel using a bottom-up approach. We assume that the system is half-duplex.

The rest of this paper is organized as follows. Section II discusses the channel network structure. In Section III, we briefly introduce the CTF of P2P PLC channels using the TL theory. We derive the CTF expressions of a two-way RA PLC channel in Section IV. Numerical examples are given in Section V to verify our results. Lastly, Section VI concludes this paper.

II. Channel Network Structure

In this paper, Canate's hybrid P2P channel model is used [14]. Fig. 1 shows the simplified network layout of Canate's hybrid P2P channel model which consists of four segments between transceivers and three branches terminated with load impedances $Z_{b,1}$, $Z_{b,2}$ and $Z_{b,3}$.

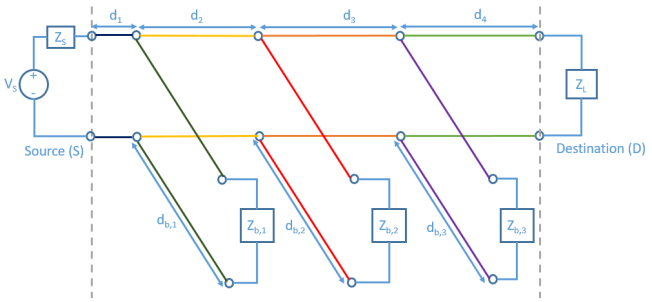

Fig. 1. Canate's channel model

In each segment, a power cable pair is included where it is characterized by its type based on the parameters and length. Table I shows five commonly used cables and their characteristics. Note that in Table I, ε_{eq} and Z_0 are the relative permittivity of the material and characteristic impedance, respectively. R, L, C, G are the per-unit-length resistance (Ω/m), inductance (H/m), capacitance (F/m), and conductance (S/m), respectively.

For simplicity, we assume that the three loads have constant impedances. Table II summarizes the loads information in the topology. The frequency response of the channel between the transceivers can be calculated using the TL theory.

TABLE I
CHARACTERISTICS OF POWER CABLES [14]

Cable type index	1	2	3	4	5
$section(mm^2)$	1.5	2.5	4	6	10
ε_{eq}	1.45	1.52	1.56	1.73	2
$Z_0(\Omega)$	270	234	209	178	143
$C(pF/m)$	15	17.5	20	25	33
$F(\mu H/m)$	1.08	0.96	0.87	0.78	0.68
R_0	12	9.34	7.55	6.25	4.98
G_0	30.9	34.7	38.4	42.5	49.3
$R = R_0 10^{-5}\sqrt{f}(\Omega/m)$					
$G = 5G_0 10^{-14} 2\pi f$					

TABLE II
PARAMETERS FOR CANATE'S PLC CHANNEL MODEL

Line section	Length	Cable type	Terminated load
A Ch+Backbone 1	d_1	n_{d_1}	N/A
Branch-tap 1	$d_{b,1}$	$n_{d_{b,1}}$	$Z_{b,1}$
Backbone 2	d_2	n_{d_2}	N/A
Branch-tap 2	$d_{b,2}$	$n_{d_{b,2}}$	$Z_{b,2}$
Backbone 3	d_3	n_{d_3}	N/A
Branch-tap 3	$d_{d,3}$	$n_{d_{b,3}}$	$Z_{b,3}$
Backbone 4	d_4	n_{d_4}	N/A
Transmitting inner impedance: Z_S			
Receiving load impedance: Z_L			

III. CTF FOR P2P PLC CHANNEL

A. ABCD Matrix

The calculation of the P2P CTF of the PLC channel is made conveniently through the use of ABCD representation of a two-port circuit as follows (see Fig. 2) [15], [16]

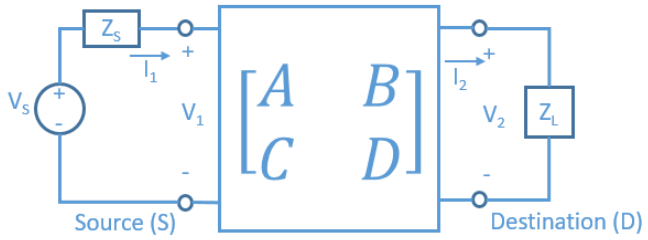

Fig. 2. Two-port network of a P2P PLC system

$$\begin{bmatrix} V_1 \\ I_1 \end{bmatrix} = \begin{bmatrix} A & B \\ C & D \end{bmatrix} \begin{bmatrix} V_2 \\ I_2 \end{bmatrix}. \tag{1}$$

Here are some common circuit configurations and their ABCD representations.

- A transmitter with voltage source, V_S and a inner impedance of source, Z_S gives the ABCD matrix

$$\Phi_S = \begin{bmatrix} 1 & Z_S \\ 0 & 1 \end{bmatrix}. \tag{2}$$

- A general impedance between the cables, Z gives the matrix

$$\Phi_Z = \begin{bmatrix} 1 & 0 \\ \frac{1}{Z} & 1 \end{bmatrix}. \tag{3}$$

- The ABCD matrix of two cascaded circuits is the product of two individual ABCD matrix, i.e Φ_1 and Φ_2.

$$\Phi_0 = \Phi_1 \Phi_2, \tag{4}$$

$$\begin{bmatrix} A_0 & B_0 \\ C_0 & D_0 \end{bmatrix} = \begin{bmatrix} A_1 & B_1 \\ C_1 & D_1 \end{bmatrix} \begin{bmatrix} A_2 & B_2 \\ C_2 & D_2 \end{bmatrix}. \tag{5}$$

- A cable line with characteristic impedance, Z_0 and propagation constant,γ and length, d gives the matrix

$$\Phi_C = \begin{bmatrix} \cosh(\gamma d) & Z_0 \sinh(\gamma d) \\ \frac{1}{Z_0}\sinh(\gamma d) & \cosh(\gamma d) \end{bmatrix}. \tag{6}$$

B. Equivalent Input Impedance

For any two-port network with load impedance, Z_L the equivalent input impedance, Z_{eqb} can be derived using its ABCD representation as follows

$$Z_{eqb} = \frac{V_1}{I_1} = \frac{AZ_L + B}{CZ_L + D}. \tag{7}$$

C. CTF for PLC with No Branches

The CTF between the source and the destination is given by

$$H(f) = \frac{Z_L}{AZ_L + B + CZ_L Z_S + DZ_S}. \tag{8}$$

Note that the CTF of a network depends on the inner impedance of the source, Z_S, its connected load Z_L as well as the inner ABCD parameter.

D. CTF for PLC with One Branch

The channel model of a transmission line with one branch circuit is depicted in Fig. 3. The structure is divided into three cascaded two-port network sub-circuits, i.e. the main backbone transmission line segment, Φ_1, the branched-circuit segment Φ_2, and the second backbone transmission line segment, Φ_3.

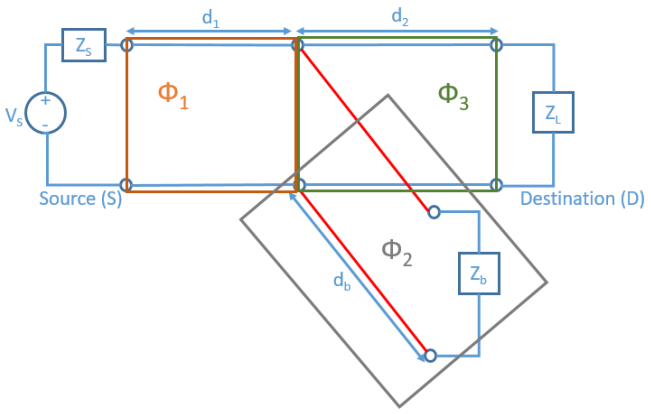

Fig. 3. A transmission line with a branch circuit

The steps for obtaining the CTF are explained as follows:

1) We calculate Φ_1, Φ_2, and Φ_3. The ABCD matrix for the backbone segment can be calculated directly. However,

for the branch segment, we need the equivalent input impedance to calculate the ABCD matrix, using (2) - (6). The results are given by

$$\Phi_1 = \begin{bmatrix} A_1 & B_1 \\ C_1 & D_1 \end{bmatrix} = \begin{bmatrix} \cosh(\gamma_1 d_1) & Z_{0,1}\sinh(\gamma_1 d_1) \\ \frac{1}{Z_{0,1}}\sinh(\gamma_1 d_1) & \cosh(\gamma_1 d_1) \end{bmatrix}. \quad (9)$$

$$\Phi_2 = \begin{bmatrix} A_b & B_b \\ C_b & D_b \end{bmatrix} = \begin{bmatrix} 1 & 0 \\ \frac{1}{Z_{eqb}} & 1 \end{bmatrix}. \quad (10)$$

$$\Phi_3 = \begin{bmatrix} A_2 & B_2 \\ C_2 & D_2 \end{bmatrix} = \begin{bmatrix} \cosh(\gamma_2 d_2) & Z_{0,2}\sinh(\gamma_2 d_2) \\ \frac{1}{Z_{0,2}}\sinh(\gamma_2 d_2) & \cosh(\gamma_2 d_2) \end{bmatrix}. \quad (11)$$

where $Z_{0,1}$, γ_1 and d_1 are the characteristic impedance, propagation constants and cable length of the first backbone segment, respectively, Z_{eqb} denotes the equivalent input impedance of branched-circuit segment, $Z_{0,2}$, γ_2 and d_2 are the characteristic impedance, propagation constants and cable length of the second backbone segment, respectively.

2) We calculate the ABCD matrix of the whole structure, Φ_T, which is the product of the ABCD matrix of each segment. The result is given by

$$\Phi_T = \prod_{i=1}^{3} \Phi_i = \begin{bmatrix} A_T & B_T \\ C_T & D_T \end{bmatrix}. \quad (12)$$

3) Finally, the CFT of the PLC channel with one branch can be calculated using (9) - (12). The result is given by

$$H_T(f) = \frac{Z_L}{A_T Z_L + B_T + C_T Z_L Z_S + D_T Z_S} \quad (13)$$

.

IV. CTF of three-node two-way RA PLC Channels

In this paper, the three-node two-way relay system depicted in Fig. 4 is proposed. The network layout of the proposed RA PLC system model is shown in Fig. 5, which is similar to Fig. 3.

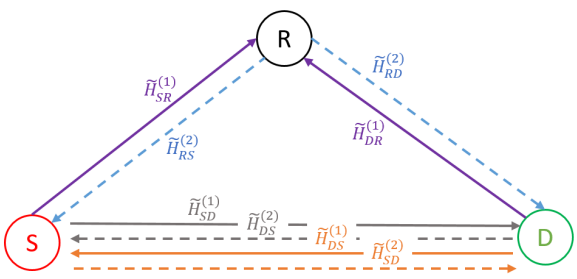

Fig. 4. A three-node two-way system model

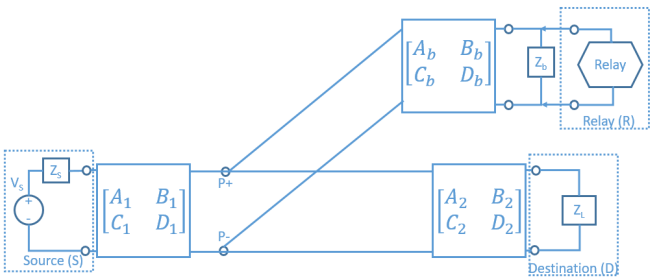

Fig. 5. Network layout of the three-segment

The transmitter in the source node consists of voltage source, V_S and a inner impedance, Z_S. The relay node works in two stages. In the first stage, the receiving relay node has a load impedance, Z_{LR}, whereas, in the second stage, the transmitting relay node has a controlled voltage source, V_R and its inner impedance Z_{SR}. Thus, the output voltage of the relay node is

$$V_R = \beta V_{LR}, \quad (14)$$

where β is the amplitude gain and V_{LR} is the received voltage of the relay node in the first phase. In the destination node, it has a load Z_L.

The CTF from S to D in the first phase, $\tilde{H}_{SD}^{(1)}$, from S to R in the first phase, $\tilde{H}_{SR}^{(1)}$, from R to D in the second phase, $\tilde{H}_{RD}^{(2)}$, from S to D in the second phase, $\tilde{H}_{SD}^{(2)}$, have been derived in [13]. Due to lack of spaces, we do not include the forward CTF derivations and results. Interested readers may see [13].

Our remaining task is to derive the reverse CTF of the RA PLC shown in Fig. 4.

A. Transfer Function from D to S in the First Phase

The relay node is treated as the load in the first phase. The CTF for the direct path, which is the signaling path from the destination to the source node along the backbone, can be found by first calculating the equivalent input impedance of the relay branch as follows

$$Z_{eqb,1} = \frac{A_b Z'_{LR} + B_b}{C_b Z'_{LR} + D_b}, \quad (15)$$

where Z'_{LR} is the equivalent impedance of Z_b parallel to Z_{LR}

$$Z'_{LR} = Z_b // Z_{LR} = \frac{Z_b Z_{LR}}{Z_b + Z_{LR}}. \quad (16)$$

Therefore, the matrix between D and S in the first phase is

$$\Phi_{DS}^{(1)} = \begin{bmatrix} A_{DS}^{(1)} & B_{DS}^{(1)} \\ C_{DS}^{(1)} & D_{DS}^{(1)} \end{bmatrix} = \begin{bmatrix} A_2 & B_2 \\ C_2 & D_2 \end{bmatrix} \begin{bmatrix} 1 & 0 \\ \frac{1}{Z_{eqb,1}} & 1 \end{bmatrix} \begin{bmatrix} A_1 & B_1 \\ C_1 & D_1 \end{bmatrix}, \quad (17)$$

where the first and the third matrices are defined in Fig. 5.

As a result, the CTF between D and S in the first phase can be expressed as

$$\tilde{H}_{DS}^{(1)} = \frac{Z_S}{A_{DS}^{(1)} Z_S + B_{DS}^{(1)} + C_{DS}^{(1)} Z_S Z_L + D_{DS}^{(1)} Z_L}. \quad (18)$$

B. Transfer Function from D to R in the First Phase

The relay node receives signal from Φ_2 to Φ_b in the first phase. Thus, the first segment, Φ_1 on the backbone is treated as branch. The equivalent input impedance of Φ_2 is formulated as

$$Z_{eqb,2} = \frac{A_1 Z_S + B_1}{C_1 Z_S + D_1}. \tag{19}$$

The matrix between D and R in the first phase is

$$\begin{aligned}\Phi_{DR}^{(1)} &= \begin{bmatrix} A_{DR}^{(1)} & B_{DR}^{(1)} \\ C_{DR}^{(1)} & D_{DR}^{(1)} \end{bmatrix} \\ &= \begin{bmatrix} A_2 & B_2 \\ C_2 & D_2 \end{bmatrix} \begin{bmatrix} 1 & 0 \\ \frac{1}{Z_{eqb,2}} & 1 \end{bmatrix} \begin{bmatrix} A_b & B_b \\ C_b & D_b \end{bmatrix},\end{aligned} \tag{20}$$

where the third matrix is defined in Fig. 5.

Thus, the CTF between D and R in the first phase is

$$\tilde{H}_{DR}^{(1)} = \frac{Z'_{LR}}{A_{DR}^{(1)} Z'_{LR} + B_{DR}^{(1)} + C_{DR}^{(1)} Z'_{LR} Z_L + D_{DR}^{(1)} Z_L}. \tag{21}$$

C. Transfer Function from D to S in the Second Phase

In the second phase, the relay node is being treated as the load. Thus, the equivalent input impedance of the relay branch is

$$Z_{eqb,3} = \frac{A_b Z''_{LR} + B_b}{C_b Z''_{LR} + D_b}, \tag{22}$$

where Z''_{LR} is the equivalent impedance of Z_b parallel to Z_{SR}

$$Z''_{LR} = Z_b // Z_{SR} = \frac{Z_b Z_{SR}}{Z_b + Z_{SR}}. \tag{23}$$

Therefore, the matrix between D and S in the second phase is

$$\begin{aligned}\Phi_{DS}^{(2)} &= \begin{bmatrix} A_{DS}^{(2)} & B_{DS}^{(2)} \\ C_{DS}^{(2)} & D_{DS}^{(2)} \end{bmatrix} \\ &= \begin{bmatrix} A_2 & B_2 \\ C_2 & D_2 \end{bmatrix} \begin{bmatrix} 1 & 0 \\ \frac{1}{Z_{eqb,3}} & 1 \end{bmatrix} \begin{bmatrix} A_1 & B_1 \\ C_1 & D_1 \end{bmatrix}\end{aligned} \tag{24}$$

Thus, the CTF between D and S in the second phase is

$$\tilde{H}_{DS}^{(2)} = \frac{Z_S}{A_{DS}^{(2)} Z_L + B_{DS}^{(2)} + C_{DS}^{(2)} Z_S Z_L + D_{DS}^{(2)} Z_L}. \tag{25}$$

D. Transfer Function from R to S in the Second Phase

In the second phase, the relay node is being treated as the transmitter. The relay node forwards signal from Φ_b to Φ_1. Thus, the first segment, Φ_2 is treated as branch. The equivalent input impedance of Φ_2 is formulated as

$$Z_{eqb,4} = \frac{A_2 Z_L + B_2}{C_2 Z_L + D_2}. \tag{26}$$

The matrix between R and S in the second phase is

$$\begin{aligned}\Phi_{RS}^{(2)} &= \begin{bmatrix} A_{RS}^{(2)} & B_{RS}^{(2)} \\ C_{RS}^{(2)} & D_{RS}^{(2)} \end{bmatrix} \\ &= \begin{bmatrix} 1 & 0 \\ Z_b & 1 \end{bmatrix} \begin{bmatrix} A_b & B_b \\ C_b & D_b \end{bmatrix} \begin{bmatrix} 1 & 0 \\ \frac{1}{Z_{eqb,4}} & 1 \end{bmatrix} \begin{bmatrix} A_1 & B_1 \\ C_1 & D_1 \end{bmatrix}\end{aligned} \tag{27}$$

Thus, the CTF between R and S in the second phase is

$$\tilde{H}_{RS}^{(2)} = \frac{Z_S}{A_{RS}^{(2)} Z_s + B_{RS}^{(2)} + C_{RS}^{(2)} Z_S Z_{SR} + D_{RS}^{(2)} Z_{SR}}. \tag{28}$$

V. Numerical Results

A simple three-node two-way topology is shown in Fig. 6 where different segments of the network used different type of cables. The complete parameters of the three-segments PLC channel realization are given in Table III.

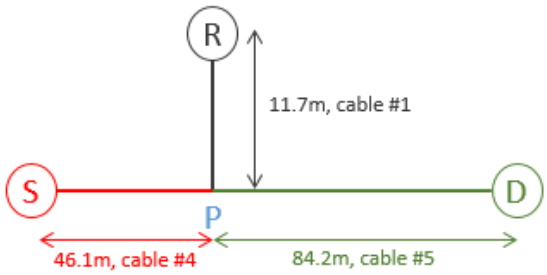

Fig. 6. Topology of a three-node two-way channel

TABLE III
PARAMETERS FOR THE THREE-SEGMENT CHANNEL REALIZATION

Line section	Length	Cable type	Terminated load
Backbone 1	$d_1 = 46.1m$	$n_{d_1} = 4$	N/A
Branch-tap 1	$d_{b,1} = 11.7m$	$n_{d_{b,1}} = 1$	$Z_1(f,T)$
Backbone 2	$d_2 = 84.2m$	$n_{d_2} = 5$	N/A
Branch-tap 2	$d_{b,2} = 0$	N/A	$Z_{b,2} = \infty$
Backbone 3	$d_3 = 0$	N/A	N/A
Branch-tap 3	$d_{d,3} = 0$	N/A	$Z_{b,3} = \infty$
Backbone 4	$d_4 = 0$	N/A	N/A
Transmitting inner impedance: $Z_S = 50\Omega$			
Receiving load impedance: $Z_L = 150\Omega$			

Meanwhile, we assume that the relay node has an inner impedance $Z_{SR} = 50\Omega$ in transmit mode and load impedance $Z_{LR} = 150\Omega$ in receive mode. The relay is attached to the branch where it has load impedance of Z_b with characteristics shown in Fig. 7.

Fig. 8 depicts the comparison of the S to D CTFs with and without relay. It can be shown that the relay greatly improves the backbone channel gain. The CTFs of the three-node two-way RA PLC appears in Fig. 9. It can be seen that

$$H_{SD} \neq \tilde{H}_{SD}^{(1)} \neq \tilde{H}_{SD}^{(2)} \tag{29}$$

$$H_{DS} \neq \tilde{H}_{DS}^{(1)} \neq \tilde{H}_{DS}^{(2)} \tag{30}$$

$$\tilde{H}_{SD}^{(1)} \neq \tilde{H}_{SR}^{(1)} \tilde{H}_{RD}^{(2)} \tag{31}$$

$$\tilde{H}_{SD}^{(2)} \neq \tilde{H}_{SR}^{(1)} \tilde{H}_{RD}^{(2)} \tag{32}$$

$$\tilde{H}_{DS}^{(1)} \neq \tilde{H}_{DR}^{(1)} \tilde{H}_{RS}^{(2)} \tag{33}$$

$$\tilde{H}_{DS}^{(2)} \neq \tilde{H}_{DR}^{(1)} \tilde{H}_{RS}^{(2)} \tag{34}$$

Justification of the forward channel CTFs has been shown in [13] by comparing the numerical results with the experimental result. As we use the same methodology to derive the reverse channel CTFs, we can also justify our numerical results.

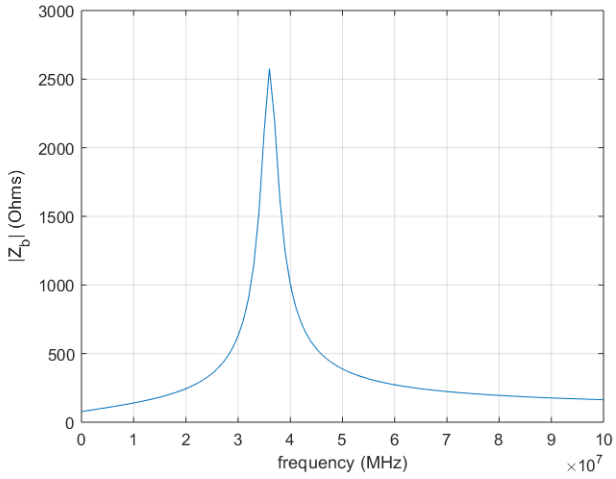

Fig. 7. Frequency response of $Z_b(f)$

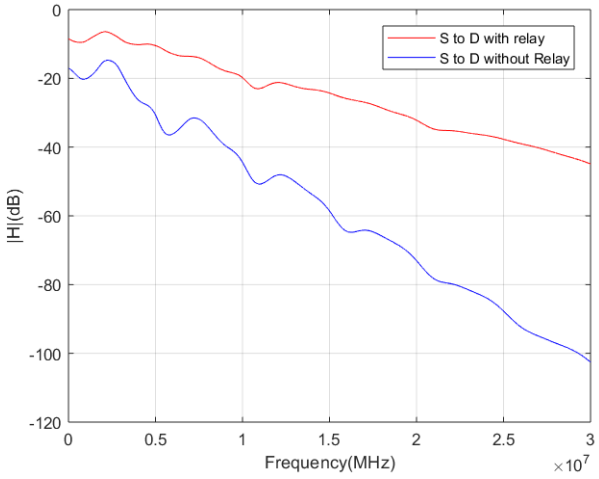

Fig. 8. CTF of S to D with and without Relay

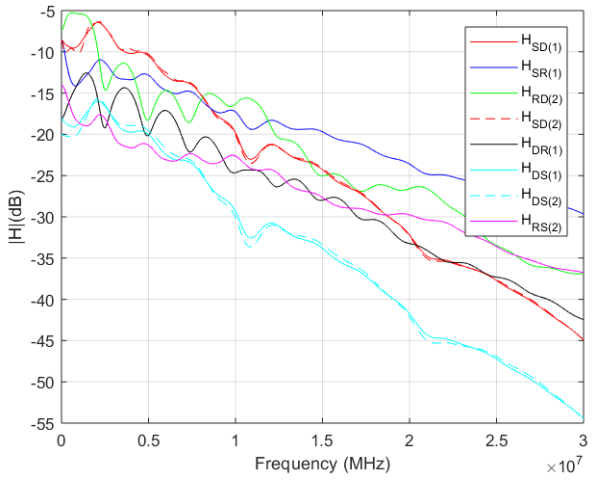

Fig. 9. CTF of a three-hop two-way relay system

As previously mentioned, we will show that the path gains in the RA PLC are correlated to each other. Let $\{x_1, \cdots, x_8\}$ be the magnitude of the two-way path gains $\{H_{SD}^{(1)}, H_{SR}^{(1)}, H_{RD}^{(2)}, H_{SD}^{(2)}, H_{DR}^{(1)}, H_{DS}^{(1)}, H_{DS}^{(2)}, H_{RS}^{(2)}\}$. Note that $\{x_1, \cdots, x_4\}$ and $\{x_5, \cdots, x_8\}$ denote the magnitude of the forward and reverse channels, respectively. The average degree of correlation is given by [13]

$$d = \sqrt{\frac{\sum_{i,j}(\rho_{i,j})^2}{N_\rho}}, \tag{35}$$

for $i > j$ and $i, j = 1, \cdots, 8$, where N_ρ is the number of $\rho_{i,j}$ and

$$\rho_{i,j} = \frac{Cov(x_i, x_j)}{STD(x_i)STD(x_j)}. \tag{36}$$

In (36), $Cov(\cdot)$ and $STD(\cdot)$ denote the covariance and standard deviation, repectively.

The average degree of correlation of forward, reverse, and two-way channels are 0.9047, 0.9242, and 0.9261, respectively. This shows that the channels are highly correlated to each other.

VI. Conclusion

A channel model of a three-node two-way RA PLC system has been proposed. Different from RA wireless system, PLC channels have high correlation among the paths. The CTF of each signaling path is affected when there is a branched circuit connection, including the relay device. The ABCD method has been applied for deriving the CTFs of the proposed RA PLC channel. It has been discussed that the CTFs of the RA PLC channels can be found by dividing them into group of an equivalent P2P PLC channels, not simply multiplying the ABCD matrix of the independent P2P PLC channels. Further, we have shown that our approach is a straight forward application to verify the Canate's PLC channel model.

Acknowledgment

This work was supported by Fundamental Research Grant Scheme (FRGS) from Ministry of Higher Education Malaysia under FRGS/1/2016/TK04/CURTIN/02/1.

References

[1] Z. Fan, P. Kulkarni, S. Gormus, C. Efthymiou, G. Kalogridis, M. Sooriyabandara, Z. Zhu, S. Lambotharan, and W. H. Chin, "Smart grid communications: Overview of research challenges, solutions, and standardization activities," *IEEE Commun. Surveys Tuts.*, vol. 15, no. 1, pp. 21–38, Jan. 2013.

[2] L. d. M. B. A. Dib, V. Fernandes, M. de L. Filomeno, and M. V. Ribeiro, "Hybrid PLC/wireless communication for smart grids and internet of things applications," *IEEE Internet Things J.*, vol. 5, no. 2, pp. 655–667, Apr. 2018.

[3] F. H. Juwono, Q. Guo, D. D. Huang, Y. Chen, L. Xu, and K. P. Wong, "On the performance of blanking nonlinearity in real–valued OFDM–based PLC," *IEEE Trans. Smart Grid*, vol. 9, no. 1, pp. 449–457, Jan. 2018.

[4] A. A. Amarsingh, H. A. Latchman, and D. Yang, "Narrowband power line communications: Enabling the smart grid," *IEEE Potentials*, vol. 33, no. 1, pp. 16–21, Jan. 2014.

[5] Y. Gong, S. Fan, L. Luo, and X. Liu, "Research on the online monitoring data transmission technology based on beidou communication," in *Proc. IEEE 18th Int. Conf. on Commun. Technol. (ICCT)*, Chongqing,China, Oct. 2018, pp. 660–663.

[6] M. Biagi, S. Greco, and L. Lampe, "Geo-routing algorithms and protocols for power line communications in smart grids," *IEEE Trans. Smart Grid*, vol. 9, no. 2, pp. 1472–1481, Mar. 2018.

[7] S. Galli, A. Scaglione, and Z. Wang, "For the grid and through the grid: The role of power line communications in the smart grid," in *Proc. of IEEE*, vol. 99, no. 6, Jun 2011, pp. 998–1027.

[8] A. K. P. Kovendan and D. Sridharan, "Design of power line communication based ICT for smart grids," in *Proc. IEEE Int. Conf. on Recent Trends in Electron. Inf. Commun. Technol. (RTEICT)*, Bangalore, India, May 2016, pp. 1452–1455.

[9] A. Ikpehai, B. Adebisi, K. M. Rabie, M. Fernando, and A. Wells, "Energy–efficient vector OFDM PLC systems with dynamic peak–based threshold estimation," *IEEE Access*, vol. 5, pp. 10 723–10 733, 2017.

[10] S. K. Mohanty and R. K. Giri, "Measurement of channel characteristic by bottom–up approach for indoor PLC channel," in *Proc. TENCON 2014 - 2014 IEEE Region 10 Conference*, Bangkok, Thailand, Oct. 2014, pp. 1–6.

[11] A. M. Tonello and F. Versolatto, "Bottom-up statistical PLC channel modeling-Part I: Random topology model and efficient transfer function computation," *IEEE Trans. Power Del.*, vol. 26, no. 2, pp. 891–898, Apr. 2011.

[12] X. Wu and Y. Rong, "Optimal power allocation for non-regenerative multicarrier relay-assisted PLC systems with QoS constraints," in *Proc. IEEE Int. Symp. on Power Line Commun. and Its Appl. (ISPLC)*, Austin, TX, USA, Mar. 2015, pp. 142–147.

[13] X. Wu, B. Zhu, and Y. Rong, "Channel model proposal for indoor relay–assisted power line communications," *IET Communications*, vol. 12, no. 10, pp. 1236–1244, Jun. 2018.

[14] F. J. Canete, J. A. Cortes, L. Diez, and J. T. Entrambasaguas, "A channel model proposal for indoor power line communications," *IEEE Commun. Mag.*, vol. 49, no. 12, pp. 166–174, 2011.

[15] D. M. Pozar, *Microwave engineering*. Hoboken, NJ: Wiley, 2012, vol. 4.

[16] T. Esmailian, F. R. Kschischang, and P. G. Gulak, "In-building power lines as high-speed communication channels: channel characterization and a test channel ensemble," *Int. J. of Communication Systems*, pp. 381–400, 2003.